Indian J. Phys. 81 (7) 683-695 (2007)

IJP

Calculations of longitudinal form factors of *p*-shell nuclei, using enlarged model space including core-polarization effects with realistic two-body effective interaction

R A Radhi*, A K Hamoudi and K S Jassim

Department of Physics, College of Science, University of Baghdad, Baghdad, Iraq

E-mail : raadradhi@yahoo.com

Received 2 March 2007, accepted 28 June 2007

Abstract : The longitudinal form factors for electron scattering have been calculated for *p*-shell nuclei using enlarged model space includes all orbits in 1*p* and 2*s*-1*d* shells. The two-body Cohen-Kurath interaction is used for the *p*-shell orbits while Preedam-Wildenthal for the *sd*-shell orbits. The two body Milliner-Kurath interactions are used for the *psd* orbits. The two-body Kuo-normalized G-matrix between the *p*-shell orbits and the *sd*-shell orbits are adopted. Core-polarization effects are taken into consideration through excitations of nucleons from the 1*s* core orbits and also from the valence 1*p* and 2*s*-1*d* orbits into higher shells, with $6\hbar\omega$ excitations. The two-body Michigan three Yakawa (M3Y) interaction is used for the core-polarization matrix elements. Core-polarization effects improve the agreement with the experimental data remarkably well and play an essential role for electromagnetic transitions and electron scattering form factors.

Keywords : *p*-shell nuclei, (*e*,*e*) elastic and (*e*,*e'*) inelastic longitudinal form factors. Calculations with enlarged model space including core-polarization effects.

PACS Nos. : 25.30.Bf, 25.30.Dh, 21.60.Cs, 27.30.+n

1. Introduction

Shell model predictions of transition strengths and form factors often under predict the experimental data for electric quadrupole (C2) excitations, by about a factor of 2 or more. It has long been recognized [1] that these transitions have highly collective properties. These collective properties can be supplemented to the usual shell model treatment by allowing excitations from the core into the model space or higher orbits, and from the model space orbits into higher orbits. The conventional approach to supplying this added ingredient to shell model wave functions is to redefine the properties of the valence nucleons from those exhibited by actual nucleons in free

*Corresponding Author

space to model-effective values [2]. Also this can be treated by connecting the ground state to the J-multipole $n\hbar\omega$ giant resonances [2], where the shape of the transition densities for these excitations is given by Tassie [3]. An alternative approach is to use a microscopic theory that allows one particle-one hole ($1p$–$1h$) excitations of the core and also of the model space to describe these longitudinal excitations.

A microscopic model has been recently [4] used to study the first order core-polarization (CP) effect on C2 form factors of p-shell nuclei. Those calculations depend on the modified surface delta interaction (MSDI) as a residual interaction to generate the core-polarization matrix elements that must be added to the model-space matrix elements. The parameters of the MSDI interaction are empirically estimated by comparing the calculated quadrupole C2 transition rate (B(C2)) with the measured values. The results are quite successful and describe the data very well in both the transition strengths and momentum transfer dependence.

The purpose of the present work is to consider the particle-hole excitations of the core and the model space to calculate the longitudinal form factors for electron scattering from p-shell nuclei. The model space in the present work is extended to include the sd-shell orbits, to become $1p_{3/2}$, $1p_{1/2}$, $1d_{5/2}$, $2s_{1/2}$ and $1d_{3/2}$ orbits. This model space is usually called psd-model space [5]. This extension in the model space will allow $2s1d$ admixture and could modify appreciably the deduced matrix elements. A more realistic nucleon-nucleon interaction is adopted in the present work for core polarization calculations which is called the Michigan Three Yukawa (M3Y) realistic two-body interaction [6] where its parameters are adjusted from the nucleon-nucleon scattering data. So, we do not adjust any parameters in the calculations of the various matrix elements. Calculations are presented for ^{6}Li, ^{7}Li, ^{10}B, ^{12}C, ^{13}C and ^{15}N.

2. Theory

The psd model space includes $1p_{3/2}$, $1p_{1/2}$, $1d_{5/2}$, $2s_{1/2}$ and $1d_{3/2}$ valence orbits. The psd Hamiltonian depends upon four types of two-body matrix elements [5],

$\langle p,p|V|p,p\rangle$ Cohn-Kurath (CKPOT) interaction [7],

$\langle sd,sd|V|sd,sd\rangle$ Preedom-Wildenthal (PW) interaction [8],

$\langle p,sd|V|p,sd\rangle$ Millener-Kurath (MK) interaction [9],

$\langle p,p|V|sd,sd\rangle$ Suzuki and Otsuka (Kuo renormalized G matrix) [10].

The reduced matrix element of the electron scattering operator $\hat{T}_\Lambda$ is expressed as the sum of the porduct of the elements of the one-body density matrix (OBDM) $X^{\Lambda}_{\Gamma_f\Gamma_i}(\alpha,\beta)$ times the single-particle matrix elements, and is given by

$$\left(\Gamma_f\left\|\hat{T}_\Lambda\right\|\Gamma_i\right)=\sum_{\alpha\beta}X^{\Lambda}_{\Gamma_f\Gamma_i}(\alpha,\beta)\left(\alpha\left\|\hat{T}_\Lambda\right\|\beta\right), \tag{1}$$

where α and β label single-particle states (isospin is included) for the *psd*-shell model space, The states $|\Gamma_i\rangle$ and $|\Gamma_f\rangle$ are described by the model space wave functions. Greek symbols are used to denote quantum numbers in coordinate space and isospace *i.e.* $\Gamma_i \equiv J_i T_i$, $\Gamma_f \equiv J_f T_f$ and $\Lambda \equiv JT$. According to the first-order perturbation theory, the single particle matrix element is given by [11]

$$\left\langle \alpha \left\| \hat{T}_\Lambda \right\| \beta \right\rangle = \left\langle \alpha \left\| \hat{T}_\Lambda \right\| \beta \right\rangle + \left\langle \alpha \left\| \hat{T}_\Lambda \frac{Q}{E_i - H_0} V_{\text{res}} \right\| \beta \right\rangle + \left\langle \alpha \left\| V_{\text{res}} \frac{Q}{E_f - H_0} \hat{T}_\Lambda \right\| \beta \right\rangle . \tag{2}$$

The first term is the zero-order contribution. The second and third terms are the core polarization contributions. The operator Q is the projection operator onto the space outside the model space.

The core-polarization terms given in eq. (2) are written as [11]

$$\sum_{\alpha_1 \alpha_2 \Gamma} \frac{(-1)^{\beta+\alpha_2+\Gamma}}{e_\beta - e_\alpha - e_{\alpha_1} - e_{\alpha_2}} (2\Gamma+1) \begin{Bmatrix} \alpha & \beta & \Lambda \\ \alpha_2 & \alpha_1 & \Gamma \end{Bmatrix} \sqrt{(1+\delta_{\alpha_1\alpha})(1+\delta_{\alpha_2\beta})}$$

$$\times \langle \alpha\alpha_1 | V_{\text{res}} | \beta\alpha_2 \rangle_\Gamma \left\langle \alpha_2 \left\| \hat{T}_\Lambda \right\| \alpha_1 \right\rangle$$

+ terms with α_1 and α_2 exchanged with an over all minus sign, (3)

where the index α_1 runs over particle states and α_2 over hole states e is the single-particle energy, and is calculated according to [11]

$$e_{n\ell j} = (2n + \ell - 1/2)\hbar\omega + \begin{Bmatrix} -1/2(\ell+1)\langle f(r)\rangle_{n\ell} & \text{for } j = \ell - 1/2 \\ 1/2\ell\langle f(r)\rangle_{n\ell} & \text{for } j = \ell + 1/2 \end{Bmatrix} \tag{4}$$

with $\langle f(r)\rangle_{n\ell} \simeq -20A^{-2/3}$ and $\hbar\omega = 45A^{-1/3} - 25A^{-2/3}$

The single particle matrix elements reduced in both spin and isospin, is written in terms of the single-particle matrix elements reduced in spin only [11]

$$\left\langle \alpha_2 \left\| \hat{T}_\Lambda \right\| \alpha_1 \right\rangle = \sqrt{\frac{2T+1}{2}} \sum_{t_z} l_T(t_z) \left\langle j_2 \left\| \hat{T}_{jt_z} \right\| j_1 \right\rangle , \tag{5}$$

with

$$l_T(t_z) = \begin{cases} 1 & \text{for } T = 0 \\ (-1)^{1/2 - t_z} & \text{for } T = 1 \end{cases}, \tag{6}$$

where t_z = 1/2 for a proton and −1/2 for a neutron.

Core-polarization effects are taken into consideration through $1p$-$1h$ excitations from $1s$ core orbits into higher orbits and excitations are also considered from $1p$ and $2s1d$ model space orbits into higher orbits. All excitations are considered up to $6\hbar\omega$ excitations. For the residual two-body interaction V_{res}, the M3Y interaction of Bertch

et al. [6] is adopted. The interaction is taken between a nucleon in any core-orbits and a nucleon that is excited to higher orbits with the same parity and with the required multipolarity (Λ), and also between a nucleon in any *psd* orbits and that is excited to higher orbits with the same parity and with the required multipolarity. The form of the potential is defined in eqs. (1)-(3) in Ref. [6]. The parameters of 'Elliot' are used which are given in Table 1 of the mentioned reference. A transformation between *LS* and *jj* is used to get the relation between the two-body shell model matrix elements and the relative and center of mass coordinate, using the harmonic oscillator radial wave functions with Talmi-Moshinsky transformation.

The reduced single-particle matrix element of the Coulomb operator is given by [12].

$$\left\langle j_2 \left\| \hat{T}_J \right\| J_1 \right\rangle = \int_0^\infty dr r^2 j_J(qr) \left\langle j_2 \left\| Y_J \right\| J_1 \right\rangle R_{n_1\ell_1}(r) R_{n_2\ell_2}(r) \tag{7}$$

where $j_J(qr)$ is the spherical Bessel function and $R_{n\ell}(r)$ is the single-particle radial wave fuction.

Electron scattering longitudinal (Coulomb) form factor involving angular momentum J and momentum transfer q, between initial and final nuclear shell model states of spin $J_{i,f}$ and isospin $T_{i,f}$ are [13]

$$\left|F_{CJ}(q)\right|^2 = \frac{4\pi}{Z^2(2J_i+1)} \left| \sum_{T=0,1} \begin{pmatrix} T_f & TT_i \\ -T_z & 0T_z \end{pmatrix} \left(J_f T_f \left\| \hat{T}_{JT} \right\| J_i T_i \right) \right|^2 F_{cm}^2(q) F_{fs}^2(q) \tag{8}$$

where T_z is given by $T_z = (Z - N)/2$. The nucleon finite size (*fs*) form factor is $F_{fs}(q) = \mathrm{Exp}(-0.43q^2/A)$ and $F_{cm}(q) = \mathrm{Exp}(q^2b^2/4A)$ is the correction for the lack of translational invariance in the shell model (center of mass correction), where A is the mass number and b is the harmonic oscillator size parameter.

The total longitudinal form factor is given by

$$\left|F_C(q)\right|^2 = \sum_{J\geq 0} \left|F_{CJ}(q)\right|^2 \tag{9}$$

3. Results and discussion

Calculations are presented for different states in different nuclei in the *p*-shell, using the *psd* model space to generate the OBDM elements $X^{\Lambda}_{T,T_z}(\alpha,\beta)$ given in eq. (1). These elements are calculated using the shell model code OXBASH [14]. Four types of two-body matrix elements are used, which are mentioned earlier in the theory. These matrix elements are supplied by the code OXBASH. The core-polarization single-particle matrix elements are calculated according to eq. (3). The many-particle matrix element that includes both the *psd* model and the core polarization effects are calculated according to eq. (1). Finally, the nuclear form factor can be obtained from eqs. (8) and (9). The

single-particle wave functions are those of the HO potential with size parameter b, chosen to reproduce the root mean square charge radius. For higher q-values, Woods-Saxon (WS) potential is used for some cases for comparison.

3.1. The nucleus ^6Li :

Figure 1 represents the longitudinal form factors for the transition from the ground state (1^+0) to the state 3^+0 at 2.18 MeV. The size parameter is taken to be 1.88 fm [15].

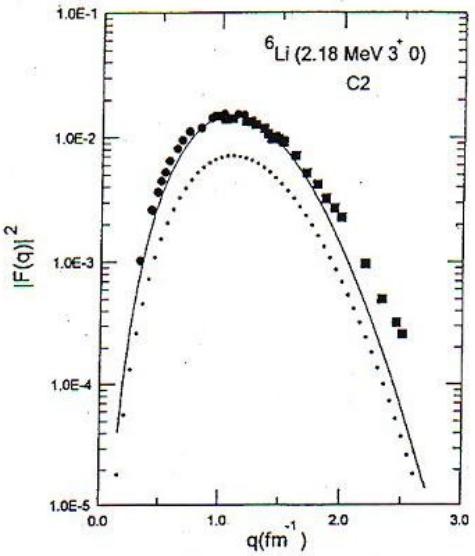

Figure 1. The longitudinal C2 form factors for the isoscalar transition to the 3^+ (2.18 MeV) state in ^{6}Li. The dotted curve represents the calculation with the *psd* model space alone and the solid curve represents the calculation that includes core-polarization effect. The data are taken from Ref. [16] (circles) and Ref. [17] (squares).

The dotted curve represents the calculations using the *psd* wave functions without CP effects. The solid curve represents the calculations that include core-polarization effects. The experimental data are taken from Refs. [16] and [17]. Including CP effects enhance the form factor appreciably and describe the experimental data extremely well for $q \leq 2$ fm^{-1}. The missing C2 strength observed in the restricted enlarged model space (*psd*) is largely compensated for by including CP effects. The contribution of the C4 multipole, which is absent in the 1*p*-shell model calculations [4], is rather small and has a negligible effect on the total form factor. Extending the 1*p*-shell - model space does not affect the longitudinal form factor, and the main effects are due to CP. However, the high q-C2 multipole seems to lack some strength. Previous calculations [4] give more agreement with the high q data than that presented here. However, in Ref [4], the MSDI is used where the parameters are fitted to each nucleus separately, and the fitted parameters compensate for the missing strength. The CP calculation still depends on the poorly understood effective interaction in light nuclei. The realistic M3Y interaction used in present work depends on the free nucleon-nucleon scattering data.

So, it still needs more efforts to find a reasonable residual interaction that obey the nuclear physics requirements and give more understanding to nuclear structure studies.

3.2. The nucleus ^7Li :

Calculations are presented for the transitions from the ground state (3/2$^-$1/2) to the 1/2$^-$1/2 state and 7/2$^-$1/2 state at 0.478 MeV and 4.53 MeV, respectively. A size parameter b = 1.77 fm is used for the HO potential [18]. The longitudinal form factors for these states are shown in Figure 2. The form factors including CP effect (solid

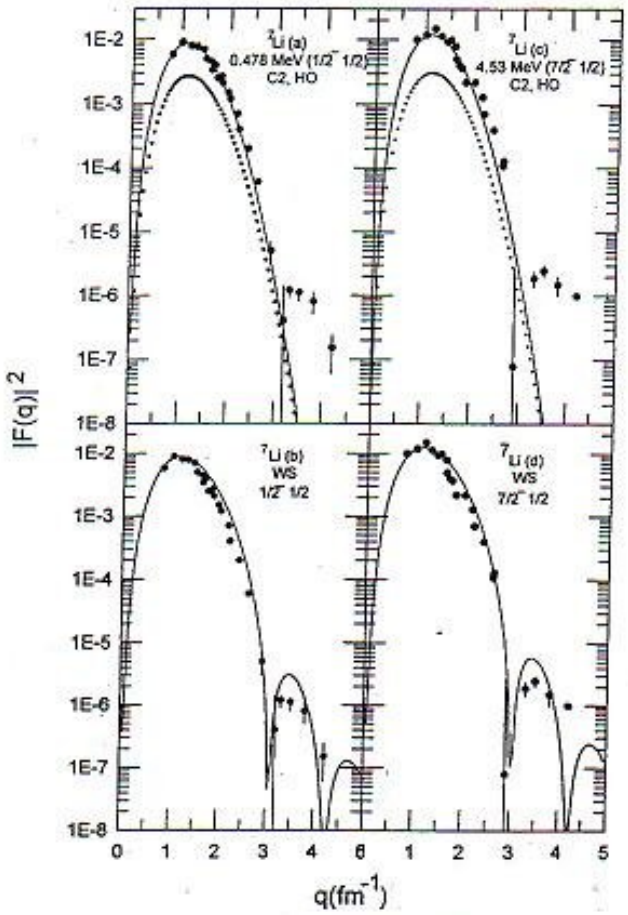

Figure 2. The longitudinal inelastic form factors for the 1/2$^-$1/2 (0.478 MeV) (a,b) and for the 7/2$^-$1/2 (4.53 MeV) (c,d) states in ^{7}Li. The dotted curves represent the calculation with *psd* model space without CP effect and the solid curves represent the calculations that include CP effect. The upper panel represents the form factors that calculated with the HO potential for the radial part of the single-particle matrix elements, while the lower panel represents those of the Woosd-Saxon potential. The data are taken from Ref. [19] for the 1/2$^-$1/2 state and from Ref. [20] for the 7/2$^-$1/2 state.

curves) in the upper panel of Figure 2(a,c) reproduce the data of Refs. [19] and [20] for the two transitions, respectively, extremely well up to $q \approx 3$ fm^{-1}. Again, the C4

contribution has negligible effect on the form factor. So, extending the model space to include the $2s1d$-shell does not modify the result. CP effect has essential contribution to explain the data. Fortunately, the experimental data are available for high q values ($q > 3$ fm^{-1}), which can be used as a stringent test for the model used. If we compare these results with other results, such as those used an enlarged model space [21], where all admixtures of $2\hbar\omega$ components are taken into account, with no inert core, we notice that their results at low q seems to lack some strength, and the large q data ($q > 3$ fm^{-1}), can not be reproduced. The low q deficiencies are remedied by introducing effective charges [22], by fitting the electric quarupole moments calculated in the $2\hbar\omega$ space, to the experimental values. The diffractive structure appeared in the experimental data for $q > 3$ fm^{-1} can not be explained in all previous calculations [23, 24], even with the inclusion of meson exchange currents (MEC). The available effective interactions used to generate the energy levels in p-shell nuclei do not alter this behavior in the form factor. Also, the residual interaction used in this work for the CP terms does not remedy this deficiency.

We repeat the calculations of the form factors for the two states mentioned above in ^{7}Li, but with Woods-Saxon potential for the single-particle matrix elements. In this case we use effective charge model to compensate for the CP effects, with $\delta e = 0.35$. The results are presented in the lower panel of Figure 2, which are labeled b and d. We notice that diffraction minima are obtained around $q = 3$ fm^{-1} and explain the diffractive structure in these two states. So, the high q data depend strongly on the radial part of the single-particle wave functions.

3.3. The nucleus ^{10}B :

The ground state of ^{10}B is $J^{\pi}T = 3^{+}0$. A wide range of experimental data ($q = 0.48 - 2.58$ fm^{-1}) is available [25] for different states in ^{10}B. Figure 3 shows the longitudinal elastic form factor. The CO form factor which is the Fourier transform of the ground state charge density is calculated with the inclusion of the occupation number of the core (^{4}He) which gives the OBDM equal to 5.2915. The C2 form factor is calculated with *psd* model space wave functions (the upper panel). The total form factor under predicts the data for $q > 1.0$ fm^{-1}. Inclusion of the CP effect enhances the C2 form factor and explains the total longitudinal experimental form factor very well through out the whole range of momentum transfer. Such agreement could not be obtained by performing calculations within a restricted $1p$-shell space and utilizing state-independent effective charges for the nucleons [26]. The size parameter of the HO potential is taken to be 1.71 fm [18] to get the single-particle wave functions. This size parameter is used for all states of ^{10}B considered in this work. Different values have been used to fit the elastic scattering form factor data [25], b= 1.65 fm for $2\hbar\omega$ calculation and b = 1.6 fm for core-polarization effect. Also b = 1.7 fm and 1.5 fm have been adopted in the work of Ref. [25] for inelastic electron scattering for $2\hbar\omega$ shell model calculations

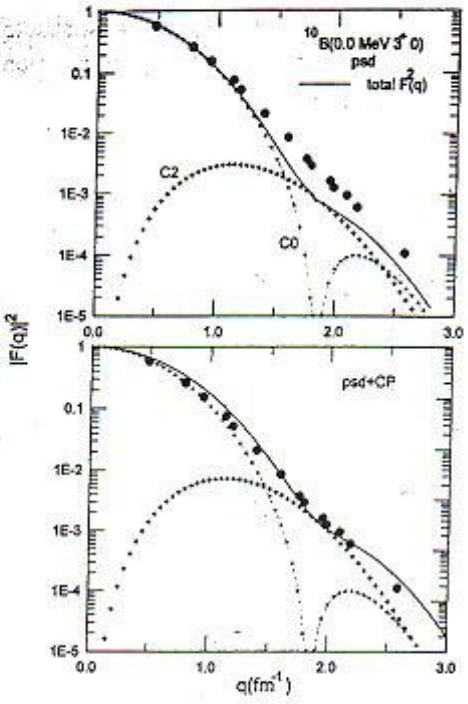

Figure 3. The elastic longitudinal form factors for ^{10}B. The upper panel represents the *psd* calculations without CP effect, and the lower panel represents those with CP effect. The data are taken from Ref. [25].

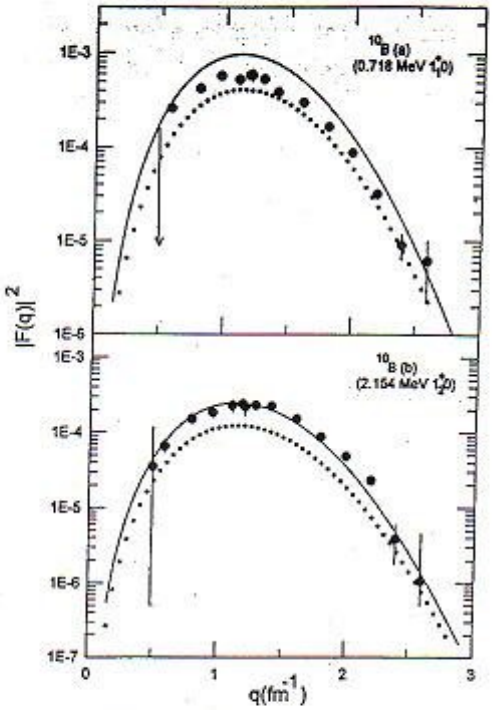

Figure 4. The inelastic longitudinal form factors for the 1+0 states at 0.718 MeV (upper panel) and 2.154 MeV (lower panel) in ^{10}B. The solid and dotted curves are the *psd* calculations with and without core-polarization effect, respectively. The data are taken from Ref. [25].

and those with core-polarization effect, respectively. Figure 4 shows the longitudinal form factors for the inelastic scattering to the 1+0 states at 0.718 MeV (upper panel) and at 2.154 MeV (lower panel). A notable result of core-polarization is to increase the form factor by a factor of more than 2 over the restricted *psd*-shell calculations in both states. The results over estimate the data for 0.718 MeV state (solid curve in the upper panel), while they explain the data remarkably well for the 2.154 MeV state (solid curve in the lower panel). The main contribution comes from the C2 component, while the C4 component has a negligible effect.

The calculations for the 2+0 states at 3.587 MeV and 5.92 MeV, are shown in Figure 5. The CP effect enhances the form factors but could not explain the data for both states. The data are well explained by the restricted *psd*-shell model space. These states might be not pure states, but mixed with other states.

Figure 6 represents the calculation for the 4+0 state at 6.025 MeV. A notable enhancement is observed with CP effect, bringing the longitudinal form factor in a

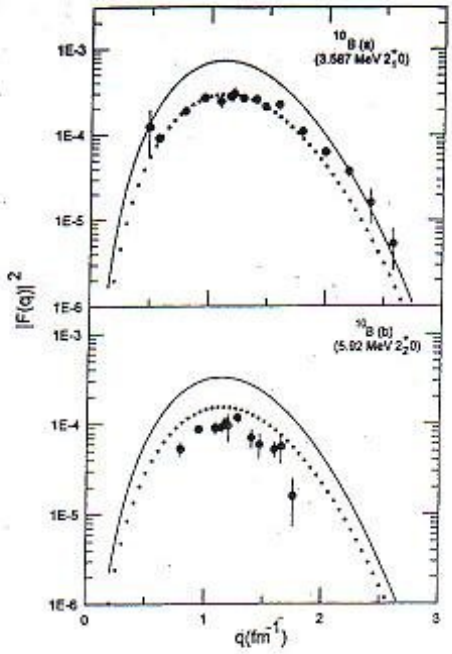

Figure 5. Same caption as to Figure 4, but for the 2⁺0 states at 3.587 MeV and 5.92 MeV.

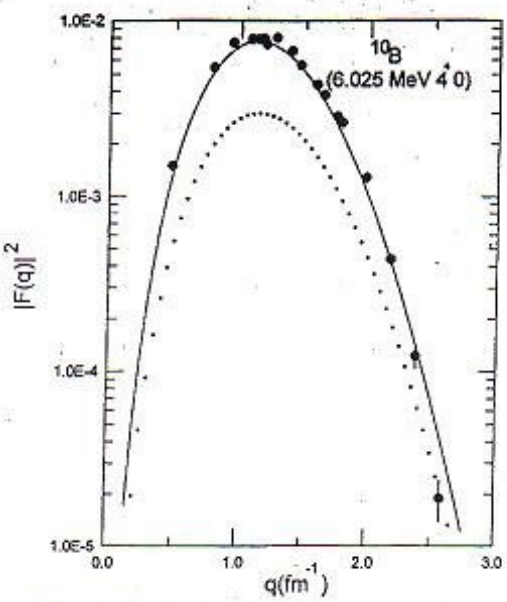

Figure 6. The inelastic form factors for the 4⁺0 state at 6.025 MeV in ^{10}B. The solid and dotted curves are the *psd* calculations with and without core-polarization effect, respectively. The data are taken from Ref. [25].

remarkable agreement with the experimental data. The $2\hbar\omega$ calculation of Cichocki *et al.* [25] under estimates the data by more than a factor of 2.

3.4. The nucleus ^{12}C :

The C2 form factors for the isoscalar transition from the 0⁺0 ground state to the 2⁺0 state at 4.439 MeV are shown in Figure 7 calculated with *psd*-shell model space with and without CP effect. The result with CP effect is closer to the data of Ref. [27] than that of the restricted *psd* result. The low q data are very well reproduced with CP calculation, and for $q \geq 1.0$ fm^{-1}, the result over predicts the data. The size parameter b = 1.64 fm is adopted [27].

3.5. The nucleus ^{13}C :

The calculations for the C2 longitudinal form factors for the transitions from the 1/2⁻1/2 ground state to the 3/2⁻1/2 states at 3.68 MeV and at 9.90 MeV and also to the 5/2⁻1/2 state at 7.53 MeV are shown in Figure 8. We employ a size parameter b = 1.64 fm for the single-particle wave functions of the HO potential [28]. The model space matrix elements are calculated with the Cohen-Kurath (CK) interaction (CKPOT) [7], where a restricted 1*p*-shell model orbits are used. The low q data for the first 3/2⁻1/2 state and for the 5/2⁻1/2 state are very well explained when CP effect is

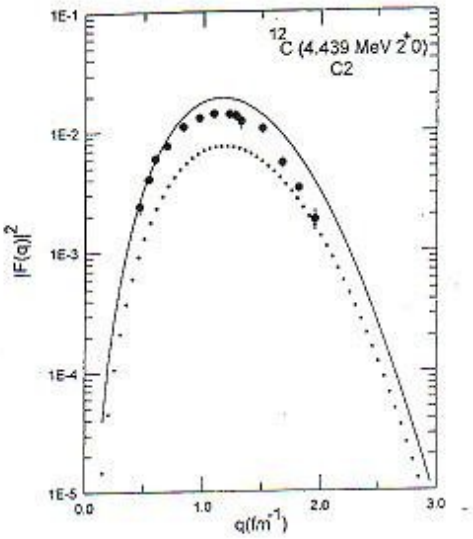

Figure 7. The inelastic C2 form factors for the 2⁺0 state at 4.439 MeV in ^{12}C. The solid and dotted curves are the *psd* calculations with and without core-polarization effect, respectively. The data are taken from Ref. [27].

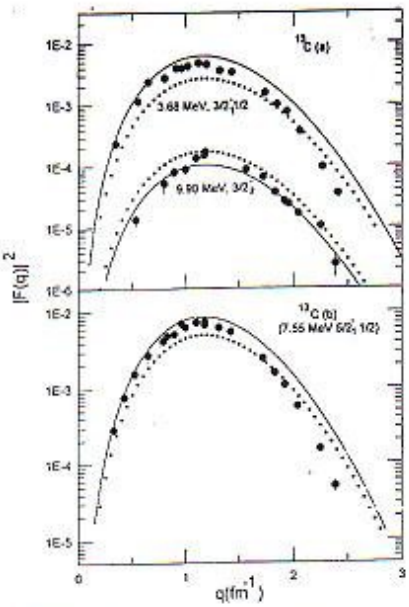

Figure 8. The inelastic longitudinal form factors for the 3/2⁻1/2 states at 3.68 MeV and 2.154 MeV (upper panel), and for the 5/2⁻1/2 state at 7.55 MeV (lower panel) in ^{13}C. The solid and dotted curves are the *psd* calculations with and without core-polarization effect, respectively. The data are taken from Ref. [28].

included and the high q data ≥ 1 fm^{-1} are over estimated. The discrepancy in the shape of the form factors for large q values can be compensated by adjusting the value of b. The effect of increasing b value is to displace the form factor to smaller q, with small decrease in magnitude and *vice versa*. However, our aim in this work is to study the core-polarization contributions without adjusting any parameter.

The second 3/2⁻1/2 state at 9.90 MeV is very well reproduced when the CP effect is included. The inclusion of CP effect for this state suppresses the C2 form factor and agrees very well with all the available experimental data. This behavior contradicts the other C2 form factors, where the CP effect enhances the form factors by about a factor of 2. This fact indicates that given the nucleons effective charges more than that of their bare charges will not always resolve the discrepancy between the theory and the experiment. So core-polarization effects should be taken into account microscopically and not by normalizing the model space matrix elements to account for the CP effect.

3.6. The nucleus ^{15}N :

The ground state of ^{15}N is of $J^\pi T$ = 1/2⁻1/2 and can be described simply by a proton hole in the $1p_{1/2}$ orbit. The form factors for the C2 transition to the 3/2⁻1/2 state at

6.32 MeV, is displayed in Figure 9, calculated with 1*p*-shell model wave functions with and without CP effect. The upper panel represents the calculation with the HO

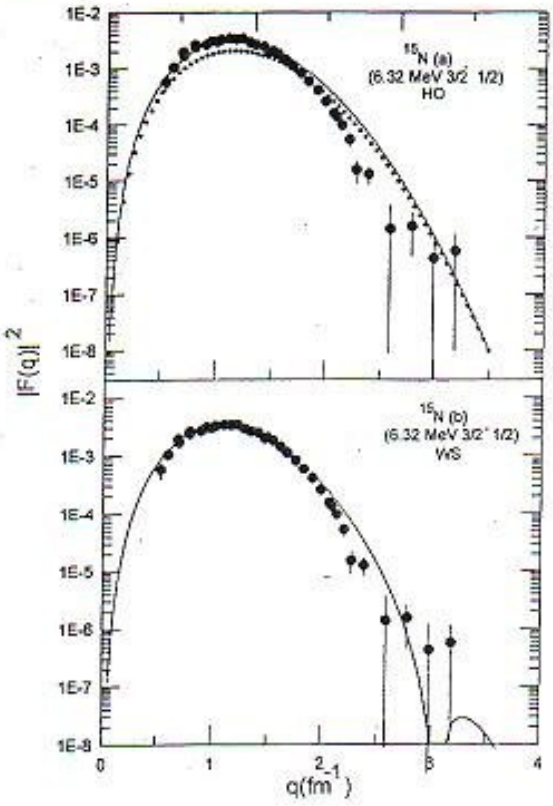

Figure 9. The longitudinal inelastic form factors for the 1/2$^-$1/2 (6.32 MeV) state in ^{15}N. The dotted curves represent the calculation with *psd* model space without CP effect and the solid curves represent the calculations that include CP effect. The upper panel represents the form factors that calculated with the HO potential for the radial part of the single-particle matrix elements, while the lower panel represents those of the Woosd-Saxon potential. The data are taken from Ref. [30].

oscillator potential for the single-particle states with b = 1.678 fm [29]. The calculation with CP effect enhances the form factor and describes the data of Ref. [30] extremely well up to $q \approx 2$ fm^{-1}. Beyond that no much difference appeared between the 1*p*-shell model result and that with CP effect. The data for $q \geq 2.5$ fm^{-1} have very large error bars, but however, they show a diffractive minimum near $q \approx 2.5$ fm^{-1}, and beyond that a second maximum appears. When the form factor is calculated with Woods-Saxon potential, using effective charge model for the core-polarization with δe = 0.35, a diffraction minimum appears at $q \approx 3$ fm^{-1}, as shown in the lower panel of Figure 9. It was pointed out [31] that calculations using more realistic nucleon wave functions obtained from a well of a finite depth, for example, the WS potential leads to an effective decrease of the form factors for $q > 3$ fm^{-1}. However, for $q < 2.5$ fm^{-1} the experimental q dependence of the form factors is described well by HO wave functions calculations [32].

4. Conclusions

Core-polarization effects are essential in the calculation of longitudinal form factors. Most of the form factors are enhanced by including core-polarization effects, but few of them are decreased, bringing the results close to the experimental data. Extending the 1*p*-shell model space to include higher shells such as 2*s*-1*d* shell, does not modify the 1*p* predictions significantly, and the C4 multipole that appears because of the extended model, has a negligible contribution. The inclusion of core-polarization effects gives a remarkable improvement in the form factors without introducing adjustable parameters. Core-polarization effects with M3Y interaction, used as a residual interaction, succeeded in describing the electron scattering data for the entire region of 1*p*-shell nuclei. The high q-data are successfully described when the radial part of the single-particle wave functions are those of the Woods-Saxon potential, rather than the harmonic oscillator potential.

Acknowledgment

The authors would like to express their thanks to Professor B A Brown of the National Superconducting Cyclotron Laboratory, Michigan State University for providing them the computer code OXBASH.

References

[1] D E Alburger, P D Parker, D J Bredin, D H Wilkinson, P F Donovan, A Gallmann, R E Pixley, L F Chase (Jr.) and R E McDonald *Phys. Rev.* **143** 692 (1966)

[2] B A Brown, R Radhi and B H Wildenthal *Phys. Rep.* **101** 313 (1983)

[3] L J Tassie *Austr. Jour. Phys.* **9** 407 (1956)

[4] R A Radhi, A A Abdullah, Z A Dakhil and N M Adeeb *Nucl. Phys.* **A696** 442 (2001)

[5] B A Browne *Progress in Particle and Nuclear Physics* **47** 517 (2001)

[6] G Bertch, J Borysowicz, H McManus and W G Love *Nucl. Phys.* **A284** 399 (1977)

[7] S Cohen and D Kuratfy *Nucl. Phys.* **A73** 1 (1965)

[8] B M Preedom and B H Wildentha *Phys. Rev.* C6 1633 (1972)

[9] D J Millener and D Kurath *Nucl. Phys.* **A255** 315 (1975)

[10] T Suzuki and T Otsuka *Phys. Rev.* **C56** 847 (1997)

[11] P J Brussaard and P W M Glaudemans *Shell Model Applications in Nuclear Spectroscopy* (Amsterdam : North Holand) (1977)

[12] T de Forest (Jr.) and J D Walecka *Adv. Phys.* **15** 1 (1966)

[13] T W Donnely and I Sick *Rev. Mod. Phys.* **56** 461 (1984)

[14] B A Brown, A Etchegoyen, N S Godwin, W D M Rae, W A Richter, W E Ormand, E K Warburton, J S Winfield, L Zhao and C H Zimmerman *MSU-NSCL report number 1289 2005 version.*

[15] F A Bumiller, F R Bbuskirk, J N Dyer and W A Manson *Phys. Rev.* **C50** 1492 (1972)

[16] J C Bergstrom and E L Tomusiak *Nucl. Phys.* **A262** 196 (1976)

[17] J C Bergstrom, U Deutschmann and Neuhausen *Nucl. Phys.* **A327** 439 (1979)

[18] E deVries *et al., At Data Nucl. Data Tables* **36** 500 (1987)

[19] J Lichtenstadt, J Alster, M A Moinester, J Dubach, R S Hicks, G A Petersonj and S Kowalskij *Phys. Lett.* **B219** 394 (1989)

[20] J Lichtenstadt, J Alster, M A Moinester, J Dubach, R S Hicks, G A Peterson and S Kowalski *Phys. Lett.* **B244** 173 (1989)

[21] J G L Booten and A G M van Hees *Nucl. Phys.* **A269** 510 (1994)

[22] A A Wolters, A G M van Hees and P N M Glaudemann *Phys. Rev.* **C42** 2062 (1990)

[23] S Karataklidis, B A Brown, K Amos and P J Dortmans *Phys. Rev.* **C55** 2826 (1997)

[24] M Unkelbach and H M Hofmann *Phys. Lett.* **B261** 211 (1991)

[25] A Cichochi, J Dubach, R S Hicks, G A Peterson, C W de Jager, H de Vries, N Kalanta-Nayestanki and T Sato *Phys. Rev.* **C51** 2406 (1995)

[26] T Sato, N Odagawa, H Ohtsubo and T S H Leej *Phys. Rev.* **C49** 776 (1994)

[27] J B Flanz, R S Hicks, R A Lidgren, A Hotta, B Parker and R C Yorky *Phys. Rev. Lett.* **41** 1642 (1978)

[28] D J Millener, D I Sober, H Carnnel, J T O'Brien, L W Fagg, S Kowalski and C F Williamson *Phys. Rev.* **C39** 14 (1989)

[29] C W de Jager, H de Vries and C de Vries *At Data Nucl. Data Tables* **14** 179 (1974)

[30] J Millener *(Private Communication) from the J W de Vries thesis* (1987)

[31] L Clauser, R J Peterson and R A Lindgren *Phys. Rev.* **C38** 589 (1988)

[32] N G Goncharova *Phys. Prt. Nuc.* **29** 319 (1998)